

Spectral contaminant identifier for off-axis integrated cavity output spectroscopy measurements of liquid water isotopes

J. Brian Leen, Elena S. F. Berman, Lindsay Liebson, and Manish Gupta

Citation: *Rev. Sci. Instrum.* **83**, 044305 (2012); doi: 10.1063/1.4704843

View online: <http://dx.doi.org/10.1063/1.4704843>

View Table of Contents: <http://rsi.aip.org/resource/1/RSINAK/v83/i4>

Published by the [American Institute of Physics](#).

Related Articles

Design and development of an automated flow injection instrument for the determination of arsenic species in natural waters

Rev. Sci. Instrum. **80**, 104101 (2009)

On the use of photothermal techniques for monitoring constructed wetlands

Rev. Sci. Instrum. **74**, 510 (2003)

A linear approach for the evolution of coherent structures in shallow mixing layers

Phys. Fluids **14**, 4105 (2002)

The magnetodynamic filters in monitoring the contaminants from polluted water systems (abstract)

J. Appl. Phys. **75**, 7187 (1994)

Additional information on *Rev. Sci. Instrum.*


Journal Homepage: <http://rsi.aip.org>

Journal Information: http://rsi.aip.org/about/about_the_journal

Top downloads: http://rsi.aip.org/features/most_downloaded

Information for Authors: <http://rsi.aip.org/authors>

ADVERTISEMENT



Special Topic Section:
PHYSICS OF CANCER

Why cancer? Why physics? [View Articles Now](#)

Spectral contaminant identifier for off-axis integrated cavity output spectroscopy measurements of liquid water isotopes

J. Brian Leen,¹ Elena S. F. Berman,¹ Lindsay Liebson,² and Manish Gupta^{1,a)}

¹Los Gatos Research, 67 East Evelyn Avenue, Suite 3, Mountain View, California 94041-1518, USA

²Department of Mechanical Engineering, Stanford University, Stanford, California 94305, USA

(Received 19 December 2011; accepted 5 April 2012; published online 26 April 2012)

Developments in cavity-enhanced absorption spectrometry have made it possible to measure water isotopes using faster, more cost-effective field-deployable instrumentation. Several groups have attempted to extend this technology to measure water extracted from plants and found that other extracted organics absorb light at frequencies similar to that absorbed by the water isotopomers, leading to $\delta^2\text{H}$ and $\delta^{18}\text{O}$ measurement errors ($\Delta\delta^2\text{H}$ and $\Delta\delta^{18}\text{O}$). In this note, the off-axis integrated cavity output spectroscopy (ICOS) spectra of stable isotopes in liquid water is analyzed to determine the presence of interfering absorbers that lead to erroneous isotope measurements. The baseline offset of the spectra is used to calculate a broadband spectral metric, m_{BB} , and the mean subtracted fit residuals in two regions of interest are used to determine a narrowband metric, m_{NB} . These metrics are used to correct for $\Delta\delta^2\text{H}$ and $\Delta\delta^{18}\text{O}$. The method was tested on 14 instruments and $\Delta\delta^{18}\text{O}$ was found to scale linearly with contaminant concentration for both narrowband (e.g., methanol) and broadband (e.g., ethanol) absorbers, while $\Delta\delta^2\text{H}$ scaled linearly with narrowband and as a polynomial with broadband absorbers. Additionally, the isotope errors scaled logarithmically with m_{NB} . Using the isotope error versus m_{NB} and m_{BB} curves, $\Delta\delta^2\text{H}$ and $\Delta\delta^{18}\text{O}$ resulting from methanol contamination were corrected to a maximum mean absolute error of 0.93 ‰ and 0.25 ‰ respectively, while $\Delta\delta^2\text{H}$ and $\Delta\delta^{18}\text{O}$ from ethanol contamination were corrected to a maximum mean absolute error of 1.22 ‰ and 0.22 ‰. Large variation between instruments indicates that the sensitivities must be calibrated for each individual isotope analyzer. These results suggest that the properly calibrated interference metrics can be used to correct for polluted samples and extend off-axis ICOS measurements of liquid water to include plant waters, soil extracts, wastewater, and alcoholic beverages. The general technique may also be extended to other laser-based analyzers including methane and carbon dioxide isotope sensors.

© 2012 American Institute of Physics. [<http://dx.doi.org/10.1063/1.4704843>]

Measurements of stable isotopes ($\delta^2\text{H}$ and $\delta^{18}\text{O}$) in liquid water are extensively used in hydrology,¹ paleoclimatology,² and medical diagnostics.³ Until recently, these measurements were made using isotope ratio mass spectrometry (IRMS). Developments in cavity-enhanced absorption spectrometry (i.e., isotope ratio infrared spectroscopy) have made it possible to measure these isotopes using faster, field-deployable instrumentation that uses fewer consumables and is more cost-effective.⁴⁻⁶ Several groups have attempted to extend the technology to measure water extracted from plants and soils.⁷⁻¹⁰ They found that other extracted organics¹¹ (methanol, ethanol, acids, glycols, and other species that co-distill with the plant water but are not removed by activated charcoal¹²) absorbed light at frequencies similar to that absorbed by the water isotopomers (near 1390 nm), leading to $\delta^2\text{H}$ and $\delta^{18}\text{O}$ measurement errors ranging up to 46.5 ‰ (Ref. 7) and 20.94 ‰ (Ref. 10), respectively.¹³

In this paper, we describe in detail a method for analyzing the off-axis ICOS spectrum of liquid water to determine the presence of interfering absorbers and correct the measured values of $\delta^2\text{H}$ and $\delta^{18}\text{O}$ accordingly. The cavity-enhanced absorption spectrum of liquid water near 1390 nm used in the Los Gatos Research liquid water isotope analyzer (LWIA) is

shown in Figure 1 and consists of large absorption features from H_2^{16}O , H_2^{18}O , and $\text{H}^2\text{H}^{16}\text{O}$. The transmission spectrum is fit to a function of the form¹⁴

$$I(\nu) = \frac{b_0 + b_1\nu + b_2\nu^2 + \dots}{1 + G(V_1 + V_2 + V_3 + \dots)}, \quad (1)$$

where ν is the relative laser frequency, $I(\nu)$ is the measured laser transmission, b_n are the baseline coefficients, G is the cavity gain factor, and V_n are Voigt functions (see Ref 15 for details on the Voigt line shape).

When methanol is added to the water, small, discrete absorption features appear between and under the large water isotopomer absorptions (see insets of Figure 1 for 100 ppm_v of methanol). Because these absorptions are not accounted for in the model of Eq. (1), the fit algorithm attempts to compensate by increasing the area of water isotopomer lines near the new methanol lines, resulting in the erroneous measurement of $\delta^2\text{H}$ and $\delta^{18}\text{O}$ ($\Delta\delta^2\text{H} = \delta^2\text{H}_{\text{actual}} - \delta^2\text{H}_{\text{measured}}$ and $\Delta\delta^{18}\text{O} = \delta^{18}\text{O}_{\text{actual}} - \delta^{18}\text{O}_{\text{measured}}$).

In contrast to molecules such as methanol which absorb in a narrow region, when ethanol is added to the water, a very broad absorption results, shifting the transmission baseline down and adding minute curvature (Figure 1, green trace). To first order, the additional broadband absorption is accounted for by the b_0 and b_1 terms of Eq. (1). In practice, b_2 and

^{a)}E-mail: m.gupta@lgrinc.com.

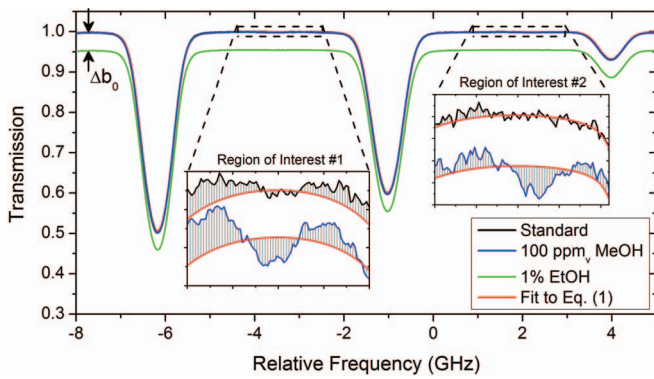


FIG. 1. Measured off-axis ICOS transmission spectra of an uncontaminated water standard, a 100 ppm_v methanol-in-water mixture (blue), and a 1% ethanol-in-water mixture (green). Insets show the non-linear, least-squares fits to the measured water standard and methanol mixture in red with residuals shown in grey. The methanol adds discrete, narrowband absorptions that can be clearly identified in the marked regions of interest. Ethanol (and larger organics) acts as a broadband absorber, which shifts the baseline offset coefficient, b_0 .

higher order terms are prescribed and the fit algorithm compensates for new curvature by changing the area of the water isotopomers' lines, again yielding erroneous measurements of $\delta^2\text{H}$ and $\delta^{18}\text{O}$. Larger alcohols and other organics containing $-\text{OH}$ functional groups behave in a manner similar to ethanol but with smaller broadband shifts (i.e., less absorption).

The errors in the measured values of $\delta^2\text{H}$ and $\delta^{18}\text{O}$ as a function of methanol and ethanol concentrations were empirically determined by adding 0–100 ppm_v methanol and 0%–2% ethanol to two internal liquid water isotope standards (Standard #1: $\delta^2\text{H} = -9.8\text{‰}$, $\delta^{18}\text{O} = -2.96\text{‰}$ and Standard #2: $\delta^2\text{H} = -154.1\text{‰}$, $\delta^{18}\text{O} = -19.57\text{‰}$) and measuring the resulting isotope ratio of contaminated samples on 14 different LWIAs. $\delta^{18}\text{O}$ measurement errors resulting from ethanol were found to scale linearly with contamination while $\delta^2\text{H}$ errors exhibit non-linear variation that was better represented using 3rd order polynomials (upper x axis in Figure 2). The measurement errors also scale linearly with the methanol concentration (shown on upper x axis in Figure 3). For all 14 instruments, the error sensitivity to changes in the ethanol and methanol concentration can be visualized from Figure 4, where the terminal ball corresponds to 100 ppm_v of methanol (plots (c) and (d)) and to 2% of ethanol (plots (a) and (b)). The instruments do not need to be calibrated for every run, but more work is needed to determine the time scale over which these sensitivities vary; the measurements in Ref 10 spanned more than two weeks with excellent results.¹⁶

Since the contaminant levels are not usually known, the measured values cannot be scaled by the methanol and ethanol concentrations. Instead, the measured spectra must be analyzed to yield metrics that can be used to identify the presence of interfering absorbers, and correct the measured isotope ratio accordingly. The cavity-enhanced transmission spectrum is analyzed to provide a broadband metric (m_{BB}) and a narrowband metric (m_{NB}) corresponding to the presence of broad, featureless interfering absorbers (e.g., ethanol and larger organics containing $-\text{OH}$ functional groups) and dis-

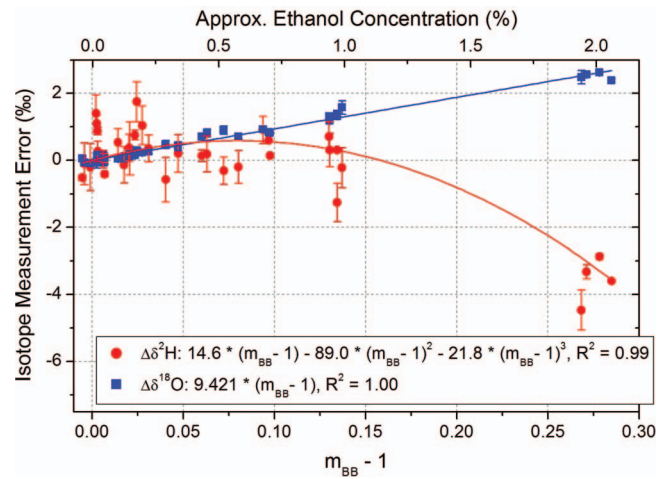


FIG. 2. $\Delta\delta^{18}\text{O}$ scales linearly with m_{BB} , whereas $\Delta\delta^2\text{H}$ follows a 3rd order polynomial. Standard #1 and Standard #2 were measured twice for each ethanol concentration (total of four points at each doping level). Data points are an average of 4 injections and error bars show the standard error of the average. Note that the data are plotted versus $(m_{BB} - 1)$ such that isotope measurement error is zero at $m_{BB} = 1$. Fits are forced through (0,0). The approximate ethanol concentration is shown on the upper x axis. Data plotted are from instrument #4.

crete, structured interfering absorbers (e.g., methanol, H_2O_2 , and CH_4).

The broadband metric for an individual sample is defined as

$$m_{BB} \equiv \frac{\bar{b}_0^s}{b_0^m}, \quad (2)$$

where \bar{b}_0^s is the average baseline offset coefficient (b_0 of Eq. (1)) for all of the water standards in the data set and b_0^m

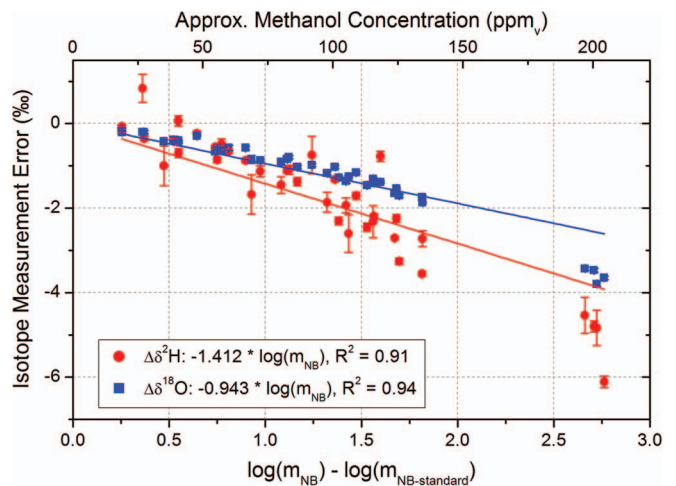


FIG. 3. $\Delta\delta^{18}\text{O}$ and $\Delta\delta^2\text{H}$ scale linearly with $\log(m_{NB})$. Standard #1 and Standard #2 were measured twice for each methanol concentration (total of four points at each doping level). Data points are an average of 4 injections and error bars show the standard error of the average. Note that the x axis zero is defined by the average $\log(m_{NB})$ value of uncontaminated water standards. Fits are forced through (0,0). For larger values of m_{NB} , a small deviation from linear behavior is visible; other groups have used a piecewise function to describe this relationship but observed a similar logarithmic trend.¹⁰ Approximate methanol concentration is shown on the upper x axis. Data plotted are from instrument #7.

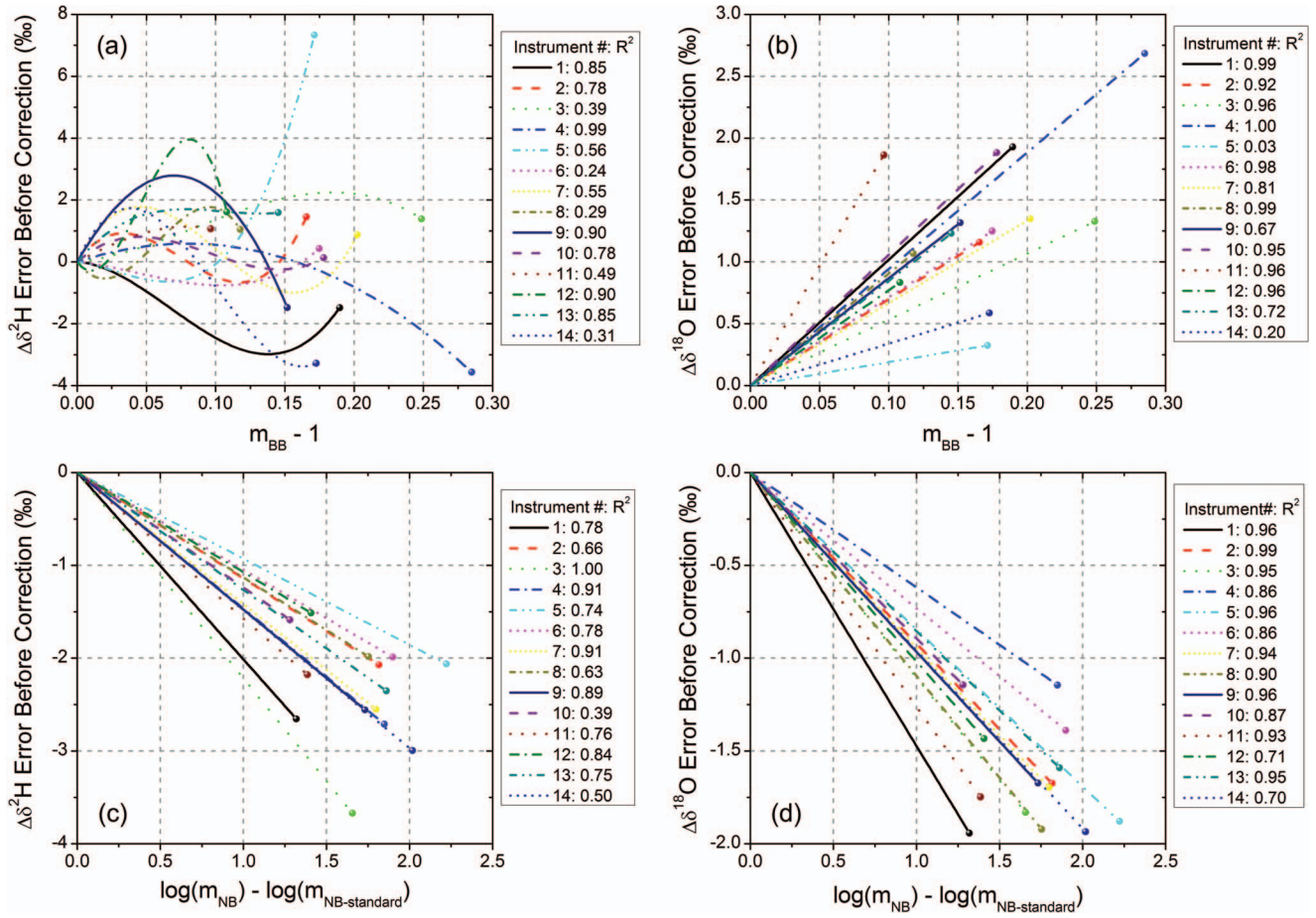


FIG. 4. Isotope error vs. metric fits for all 14 instruments: (a) 3rd order polynomial fits to $\Delta\delta^2\text{H}$ vs. $m_{BB}-1$ showing a wide variety of responses to contamination with ethanol. Poor fits (i.e., low R^2) typically have a small total deviation, indicating minimal error dependence on m_{BB} and thus ethanol contamination. (b) Linear fits to $\Delta\delta^{18}\text{O}$ vs. $m_{BB}-1$. The terminal markers in (a) and (b) correspond to 2% ethanol. (c) Linear fits to $\Delta\delta^2\text{H}$ vs. $\log(m_{NB})$. (d) Linear fits to $\Delta\delta^{18}\text{O}$ vs. $\log(m_{NB})$. The terminal markers in (c) and (d) correspond to 100 ppm_v methanol. R^2 values for each fit are shown in the legend.

is the baseline offset coefficient for the measured spectrum at hand. For uncontaminated samples, $b_0^m \simeq \bar{b}_0^s$ and $m_{BB} \simeq 1$. For samples contaminated with a broadband absorber, b_0^m is smaller than \bar{b}_0^s and $m_{BB} > 1$. Note that m_{BB} has no dependence on methanol concentration but scales linearly with ethanol concentration. \bar{b}_0^s should always be determined from the b_0 values of uncontaminated water standards (i.e., fresh water with no organic material) that are run interleaved with the unknown samples; a typical 24 h run on the LWIA will include about 30 measurements of uncontaminated water standards. The broadband metric resulting from the interleaved water standard measurements was found to have an average standard deviation of 8.2×10^{-4} within a run of 642 injections.

As shown in Figure 2, $\Delta\delta^{18}\text{O}$ scales linearly with m_{BB} , but $\Delta\delta^2\text{H}$ scales as a polynomial with m_{BB} . We have chosen a 3rd order polynomial for generality; other functional forms may be more appropriate for specific instruments. Figures 4(a) and 4(b) show the fit results to isotope errors vs. m_{BB} from 14 instruments. There are a wide variety of $\Delta\delta^2\text{H}$ responses to ethanol contamination (another example of this is found in Ref 10 (Figure 1, bottom), where the slope of $\Delta\delta^2\text{H}$ vs. m_{BB} changes at $m_{BB} = 1.2$). The large variation between instruments suggests that the sensitivity must be calibrated for

each individual isotope analyzer. Recent work on a wide variety of leaf, stem, and soil waters¹⁰ has shown that m_{BB} values are frequently below 1.1, suggesting a $\Delta\delta^{18}\text{O}$ of $\sim 0.20\text{--}2.0$ ‰ and $\Delta\delta^2\text{H} \sim -2.5\text{--}4.0$ ‰ due to broadband absorption (see Figures 4(a) and 4(b)). Using the fits in Figures 4(a) and 4(b), the $\delta^2\text{H}$ and $\delta^{18}\text{O}$ errors can be corrected by subtracting from the measured isotope ratio ($\delta^2\text{H}_{\text{measured}}$, $\delta^{18}\text{O}_{\text{measured}}$) the fit value at $m_{BB} - 1$. The results for all 14 instruments measuring water contaminated with ethanol are shown in Figure 5 (red), where the average absolute deviations from the actual isotope ratio after correction are plotted. The calculation of the average absolute deviation is equivalent to subtracting the fit from the measured values in Figure 2, taking the absolute value and averaging.

The measurement technique is substantially more sensitive to narrowband absorbers (e.g., methanol) and the narrowband metric for an individual sample is defined as

$$m_{NB} \equiv \frac{1}{N^2} \left(\sum_{\nu \in R_1} (r(\nu) - \bar{r}_1)^2 \right) \left(\sum_{\nu \in R_2} (r(\nu) - \bar{r}_2)^2 \right), \quad (3)$$

where N is total measured water number density (molecules/cm³) multiplied by 1×10^{-22} , ν is the relative laser frequency (GHz), R_n is the n -th region of interest

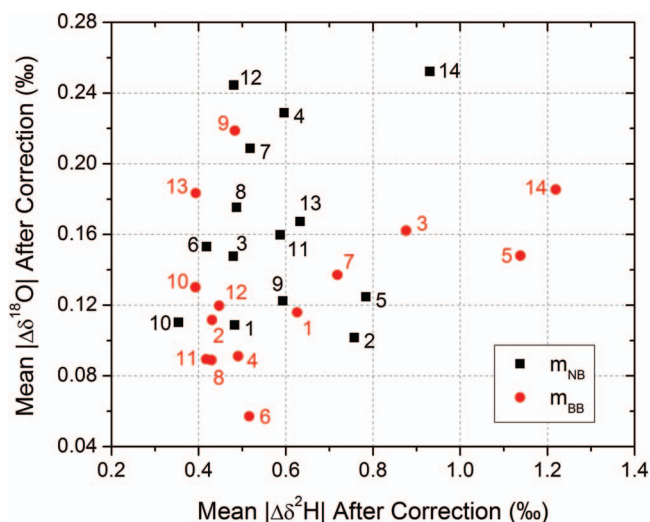


FIG. 5. Average absolute deviation after correction using the metrics described in this note. Black points were contaminated with a maximum of 100 ppm_v methanol, red points with a maximum 2% ethanol.

(identified in Figure 1), $r(\nu)$ is the fit residual at frequency ν (the difference between the measured and fit laser transmission curve at ν , shown as the grey lines in the Figure 1 insets), and \bar{r}_n is the average residual in the n -th region of interest. To calculate m_{NB} , the measured transmission spectra are first fit to the functional form in Eq. (1), the fit residuals are calculated and processed using Eq. (3). For uncontaminated water, the fit residual is limited by measurement noise. Note that m_{NB} scales logarithmically with methanol but has minimal dependence on ethanol concentration. The isotope measurement error was also determined for a single instrument as a function of H₂O₂ and CH₄ contamination. The sensitivity of $\Delta\delta^{18}\text{O}$ and $\Delta\delta^2\text{H}$ to H₂O₂ concentration was -5.95‰/‰ and -15.7‰/‰ , respectively. Likewise, the sensitivity of $\Delta\delta^{18}\text{O}$ and $\Delta\delta^2\text{H}$ to CH₄ concentration was -0.00012‰/ppm_v and 0.0048‰/ppm_v , respectively. Note that a water sample equilibrated with 1 atm of pure methane only contains $\sim 25\text{ ppm}_v$ CH₄, and $\Delta\delta^{18}\text{O}$ and $\Delta\delta^2\text{H}$ are less than -0.003‰ and 0.12‰ , respectively.

Both $\Delta\delta^{18}\text{O}$ and $\Delta\delta^2\text{H}$ scale linearly with $\log(m_{NB})$, as shown in Figure 3. Figures 4(c) and 4(d) show the distribution of linear fit results of $\Delta\delta^2\text{H}$ and $\Delta\delta^{18}\text{O}$ vs. $\log(m_{NB})$ from 14 instruments that can be used as correction curves. Note that for each instrument, the x axis has been shifted by the average $\log(m_{NB})$ measured for uncontaminated water standards. At higher contamination levels ($m_{NB} > 4000$), other groups have used a piecewise function to define this relationship;¹⁰ the deviation from a single exponential can also be accounted for by a 2nd order polynomial fit to $\log(m_{NB})$. Recent work on plant waters¹⁰ has shown m_{NB} values exceeding 9000, suggesting large measurement errors of $\Delta\delta^{18}\text{O} \sim 19\text{‰}$ and $\Delta\delta^2\text{H} \sim 17\text{‰}$ due to narrowband absorptions. Using the fits in Figures 4(c) and 4(d), the $\delta^2\text{H}$ and $\delta^{18}\text{O}$ errors can again be corrected by subtracting the fit value at $\log(m_{NB})$ from the measured isotope ratio ($\delta^2\text{H}_{\text{measured}}$, $\delta^{18}\text{O}_{\text{measured}}$). The results for all 14 instruments measuring water contaminated with methanol are shown in Figure 5 (black), where the average

absolute deviations from the actual isotope ratio after correction are plotted.

The methodology described in this paper has been implemented by Schultz *et al.*¹⁰ for a variety of leaf, stem, and soil waters. Their measured relationships between m_{BB} , m_{NB} and $\Delta\delta^{18}\text{O}$, $\Delta\delta^2\text{H}$ are consistent with those found here, and they have used these relationships to correct the measured values of $\delta^{18}\text{O}$ and $\delta^2\text{H}$. These corrected values were compared to IRMS results and the mean differences between the values ($\delta_{\text{IRMS}} - \delta_{\text{LWIA}}$) were 0.18‰ and -3.39‰ for $\delta^{18}\text{O}$ and $\delta^2\text{H}$, respectively. The difference between LWIA and IRMS $\delta^{18}\text{O}$ measurements, which used headspace equilibration with CO₂, are consistent with the convolution of the uncertainties of the IRMS and LWIA, whereas the IRMS $\delta^2\text{H}$ values, which involved chromium reduction to H₂/HD, deviate more than expected from the LWIA values. This deviation is present even for samples with minimal methanol and ethanol contamination as indicated by very small values of m_{NB} and m_{BB} . Approximately 1‰ of this shift in $\delta^2\text{H}$ is due to differences in the IRMS and LWIA as gauged on uncontaminated water standards. The remaining 2.5‰ shift is consistent with the 1–2‰ difference in $\delta^2\text{H}$ observed before and after samples are cleaned by activated charcoal.⁷ The samples in the Schultz *et al.* study were not treated with activated charcoal prior to IRMS quantification, and the difference between the IRMS and LWIA corrected values may be due to errors in the IRMS induced by combustion of other plant organics that do not perturb the LWIA measurement (e.g., larger alcohols, glycols, acids, and organics that do not contain –OH functional groups). These organics are expected to be severely depleted in $\delta^2\text{H}$ relative to the plant water,¹⁷ and even low contamination levels can lead to a few per mil offset in $\delta^2\text{H}$. Further study is needed to quantify this effect and more extensively validate the spectral contaminant identifier method for plant waters and other contaminated samples. In addition to plant waters, this method may allow for extension of the LWIA to other contaminated samples, including wastewater and alcoholic beverages. Finally, the general technique of identifying spectral contaminants using baseline offsets and narrowband absorptions may be extended to other laser-based analyzers including methane and carbon dioxide isotope sensors.

¹ *Isotope Tracers in Catchment Hydrology*, edited by C. Kendall and J. J. McDonnell (Elsevier Science B.V., Amsterdam, 1998).

² R. S. Bradley, *Paleoclimatology: Reconstructing Climates of the Quaternary* (Academic, San Diego, 1999).

³ J. Speakman, *Doubly Labelled Water - Theory and Practice* (Chapman and Hall, London, 1997).

⁴ G. Lis, L. I. Wassenaar, and M. J. Hendry, *Anal. Chem.* **80**, 287 (2008).

⁵ W. Brand, H. Geilmann, E. Crosson, and C. Rella, *Rapid Commun. Mass Spectrom.* **23**, 1879 (2009).

⁶ E. Berman, M. Gupta, C. Gabrielli, T. Garland, and J. J. McDonnell, *Water Resour. Res.* **45**, W10201, doi:10.1029/2009WR008265 (2009).

⁷ A. G. West, G. R. Goldsmith, P. D. Brooks, and T. E. Dawson, *Rapid Commun. Mass Spectrom.* **24**, 1948 (2010).

⁸ A. G. West, G. R. Goldsmith, I. Matamati, and T. E. Dawson, *Rapid Commun. Mass Spectrom.* **25**, 2268 (2011).

⁹ L. Zhao, H. Xiao, Z. Jian, L. Wang, G. Cheng, M. Zhou, L. Yin, and M. F. McCabe, *Rapid Commun. Mass Spectrom.* **25**, 3071 (2011).

¹⁰ N. M. Schultz, T. J. Griffis, X. Lee, and J. M. Baker, *Rapid Commun. Mass Spectrom.* **25**, 3360 (2011).

¹¹ A. G. West, S. Patrickson, and J. Ehleringer, *Rapid Commun. Mass Spectrom.* **20**, 1317 (2006).

¹²W. Brand, [Rapid Commun. Mass Spectrom.](#) **24**, 2687 (2010).

¹³All isotope ratios are expressed in standard notation as ‰ vs VSMOW.

¹⁴D. S. Baer, J. B. Paul, M. Gupta, and A. O'Keefe, [Appl. Phys. B.](#) **75**, 261 (2002).

¹⁵B. H. Armstrong, [J. Quant. Spectrosc. Radiat. Transf.](#) **7**, 61–88 (1967).

¹⁶N. Schultz, Department of Soil, Water, and Climate, University of Minnesota, St. Paul, MN, personal communication (2012).

¹⁷Sessions, A. L., [Geochim. Cosmochim. Acta](#) **70**, 2153 (2006).